Testing Spacecraft Formation Flying with Crazyflie Drones as Satellite Surrogates

Arturo de la Barcena*
MECE Department
University of Houston
Houston, TX 77204
adelabarcena@uh.edu

Collin Rhodes*
MECE Department
University of Houston
Houston, TX 77204
cjrhodes@cougarnet.uh.edu

John McCarroll
Matrix Research
3844 Research Blvd
Dayton, OH 45430
john.mccarroll.ext@afresearchlab.com

Marzia Cescon
MECE Department
University of Houston
Houston, TX 77204
mcescon2@central.uh.edu

Kerianne L. Hobbs
Air Force Research Laboratory
2241 Avionics Circle
Wright-Patterson AFB, OH, 45433
kerianne.hobbs@us.af.mil

Abstract—As the space domain becomes increasingly congested, autonomy is proposed as one approach to enable small numbers of human ground operators to manage large constellations of satellites and tackle more complex missions such as on-orbit or in-space servicing, assembly, and manufacturing. One of the biggest challenges in developing novel spacecraft autonomy is mechanisms to test and evaluate their performance. Testing spacecraft autonomy on-orbit can be high risk and prohibitively expensive. An alternative method is to test autonomy terrestrially using satellite surrogates such as attitude test beds on air bearings or drones for translational motion visualization. Against this background, this work develops an approach to evaluate autonomous spacecraft behavior using a surrogate platform, namely a micro-quadcopter drone developed by the Bitcraze team, the Crazyflie 2.1. The Crazyflie drones are increasingly becoming ubiquitous in flight testing labs because they are affordable, open source, readily available, and include expansion decks which allow for features such as positioning systems, distance and/or motion sensors, wireless charging, and AI capabilities. In this paper, models of Crazyflie drones are used to simulate the relative motion dynamics of spacecraft under linearized Clohessy-Wiltshire dynamics in elliptical natural motion trajectories, in pre-generated docking trajectories, and via trajectories output by neural network control systems.

TABLE OF CONTENTS

1. INTRODUCTION

The control of large constellations of satellites has seen increased attention in a variety of fields including Earth sciences and astrophysics. Commercially it has been considered for missions including space and Earth surveillance, weather forecasting, data transmission [1], and, most recently, on-orbit/in-space servicing, assembly, and manufacturing [2]. As mission complexity advances in these fields, autonomy has been introduced as a method of enabling a small number of human ground operators to manage these large satellite constellations. Autonomous satellite formation flight has been the subject of study for many years with advancements in collision avoidance [3], optimal control through trajectory tracking [4], and control through reinforcement learning [5] [6] occupying a large part of related literature over the past twenty years. Spacecraft autonomy testing, however, can be prohibitively difficult and expensive when done on orbit. It follows that the development of simple, scalable, inexpensive testing is highly desirable, with the use of terrestrial satellite surrogates being a promising method. To date, several research groups have considered using terrestrial, robotic surrogates. For instance, the authors in [7] and [8] created a remote access swarm robotarium as a robotics educational tool, and a two-dimensional representation of deep reinforcement learning controlled spacecraft was modeled on ground-based robots in [9], while [10] describes the Local Intelligent Networked Collaborative Satellites (LINCS) Lab, which employs linear quadratic regulation (LQR) control on aerial vehicles to follow satellite dynamics. This work develops an approach to simulate satellite relative motion dynamics under the linearized Clohessy-Wiltshire equations, which describe the three-dimensional motion of a chaser spacecraft with respect to a target spacecraft in the Hill's reference frame, using a surrogate platform capable of representing translational motion in three dimensions. The surrogate of choice in this paper is the Bitcraze Crazyflie 2.1 micro-quadcopter platform [11]. These drones are of interest because they are open source, inexpensive, readily available, and include up to two expansion decks which allow for features such as positioning systems, distance and/or motion sensors, wireless charging, and AI capabilities. Additionally, at 27 grams [12], their small size and affordability facilitates testing cooperative control algorithms on many vehicles in smaller lab spaces, further reducing the requirements for testing. In this work, the `gym-pybullet-drones` simulation platform [13] is leveraged as a virtual environment to simulate the Crazyflie 2.1 drones. Natural motion and controlled trajectories are determined in the space scale, then scaled and simulated in this virtual environment.

2. BACKGROUND

This section introduces how crazyflie drones can be used as a satellite surrogate test bed, the linearized relative motion spacecraft dynamics, and the dynamics and control of the

crazyflie drones.

Crazyflies as a Satellite Surrogate Test Bed

The terrestrial surrogate simulated in this paper is the Bitcraze Crazyflie 2.1 micro-quadcopter running in the `gym-pybullet-drones` gym environment [13]. The `gym-pybullet-drones` environment is an open-source, gym-style environment based on Google's Bullet Physics engine [14] using its Python binding, Pybullet, and is one of the first general purpose multi-agent Gym environments for quadcopters. The physics used to model the quadcopter is based on system identification performed on the actual Crazyflie 2.1 platform [13] and a separate study done on different physical phenomena including drag, the ground effect, and the downwash effect [15]. These inexpensive micro-quadcopters have become commonplace in lab environments and provide an easy-to-use platform for satellite formation visualization with the Crazyflies serving as scaled satellite surrogates.

Spacecraft Linearized Clohessy-Wiltshire Dynamics

A space dynamics simulator was used to create spacecraft trajectories solving the Clohessy-Wiltshire (CW) equations [16], which describe the motion of one spacecraft relative to another in the non-inertial Hill's reference frame [17], depicted in Fig. 1.
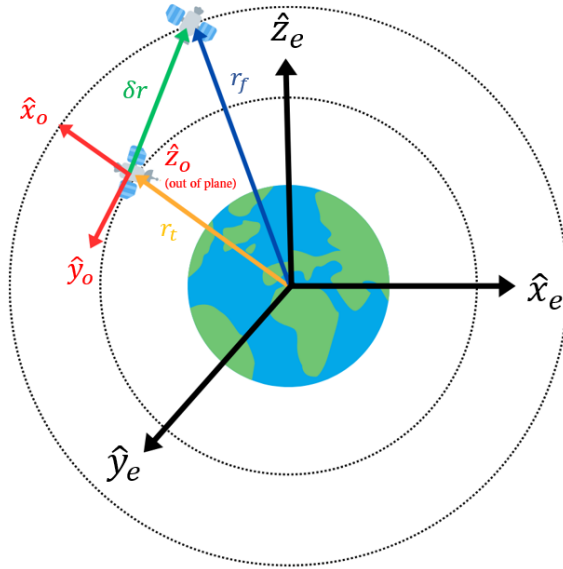
Figure 1: Earth-Centered Inertial Frame (Black) and the Non-inertial Hill's Frame (Red). The Hill's frame x-axis points from the center of the Earth to the chief satellite's center of mass, the z-axis points in the same direction as the orbital angular moment (out of the page), and the y-axis completes the orthogonal frame.

A linearization of the relative motion dynamics between the deputy and chief spacecraft is given by

$$\dot{\mathbf{x}} = A\mathbf{x} + \mathbf{B}\mathbf{u} \tag{1}$$

where,

$$A = \begin{bmatrix} 0 & 0 & 0 & 1 & 0 & 0 \\ 0 & 0 & 0 & 0 & 1 & 0 \\ 0 & 0 & 0 & 0 & 0 & 1 \\ 3n^2 & 0 & 0 & 0 & 2n & 0 \\ 0 & 0 & 0 & -2n & 0 & 0 \\ 0 & 0 & -n^2 & 0 & 0 & 0 \end{bmatrix} \tag{2}$$

and

$$B = \begin{bmatrix} 0 & 0 & 0 \\ 0 & 0 & 0 \\ 0 & 0 & 0 \\ 1/m & 0 & 0 \\ 0 & 1/m & 0 \\ 0 & 0 & 1/m \end{bmatrix} \tag{3}$$

with n representing the satellite's mean orbital motion (an inverse relationship of the orbital period) and m the satellite's mass. For Earth-based applications, $n = 0.001027$ [rad/s]. The states in this equation are given by the relative positions and velocities in the x, y, and z directions and the control is given by the thrust forces in these directions. This linearization is an approximation of the exact equations of relative motion that assumes the distance between the two satellites is much less than the distance between either satellite and the Earth, and that the chief satellite follows a perfectly circular orbit. Alternatively, these equations can be represented in discrete time [18] as using A in Eq. (4) and B defined in Eq. (5).

To create a Natural Motion Trajectory (NMT), the control law u must equal the null vector (there is no control input). The trajectory is dependant on the initial conditions (starting positions and velocities), where a relative elliptical orbit can only be ensured if

$$\dot{y}_0 = -2nx_0 \tag{6a}$$

$$y_0 = \frac{2\dot{x}_0}{n} \tag{6b}$$

These conditions arise from the closed-form solutions to the Clohessy-Wiltshire equations where the condition in Eq. (6a) ensures zero linear drift with time and Eq. (6b) ensures that there is not a constant offset to the time-dependant solution, meaning that the relative motion is centered about the target spacecraft. It should be noted that the motion out of the orbital plane, in the z direction, is completely decoupled from motion in the other two directions meaning that while an ellipse can be assured, the plane of that ellipse with respect to the orbital plane can be changed. Motion in the $x-y$ plane of the CW equations is called *in-plane* because it is in the orbital plane of the chief satellite, while any motion in the z direction is called *out-of-plane*.

Crazyflie dynamics and control model

The state space representation of the linearized dynamics of the Crazyflie 2.1 used in this work was provided in [19] and with reference to Fig. 2 is described by four decoupled subsystems as follows:

Vertical Subsystem

$$\begin{bmatrix} \Delta\dot{w} \\ \Delta\dot{z} \end{bmatrix} = \begin{bmatrix} 0 & 0 \\ 1 & 0 \end{bmatrix} \begin{bmatrix} \Delta w \\ \Delta z \end{bmatrix} + \begin{bmatrix} 1/m \\ 0 \end{bmatrix} \Delta F_z \tag{7a}$$

$$A_k = \begin{bmatrix} 4 - 3\cos(nt) & 0 & 0 & \frac{1}{n}\sin(nt) & \frac{2}{n}(1 - \cos(nt)) & 0 \\ 6(\sin(nt) - nt) & 1 & 0 & \frac{-2}{n}(1 - \cos(nt)) & \frac{1}{n}(4\sin(nt) - 3nt) & 0 \\ 0 & 0 & \cos(nt) & 0 & 0 & \frac{1}{n}\sin(nt) \\ 3n\sin(nt) & 0 & 0 & \cos(nt) & 2\sin(nt) & 0 \\ -6n(1 - \cos(nt)) & 0 & 0 & -2\sin(nt) & 4\cos(nt) - 3 & 0 \\ 0 & 0 & -n\sin(nt) & 0 & 0 & \cos(nt) \end{bmatrix} \quad (4)$$

$$B_k = \begin{bmatrix} \frac{1}{n^2}(\cos(nt) - 1) & \frac{2}{n}(t + \frac{1}{n}\sin(nt)) & 0 \\ \frac{-2}{n}(t - \frac{1}{n}\sin(nt)) & \frac{1}{n}(\frac{-4}{n}(\cos(nt) - 1) - (3n/2)t^2) & 0 \\ 0 & 0 & \frac{-1}{n^2}(\cos(nt) - 1) \\ \frac{1}{n}\sin(nt) & \frac{-2}{n}(\cos(nt) - 1) & 0 \\ \frac{2}{n}(\cos(nt) - 1) & \frac{4}{n}(\sin(nt) - 3t) & 0 \\ 0 & 0 & \frac{1}{n}\sin(nt) \end{bmatrix} \quad (5)$$

Yaw Subsystem

$$\begin{bmatrix} \Delta\dot{r} \\ \Delta\dot{\psi} \end{bmatrix} = \begin{bmatrix} 0 & 0 \\ 1 & 0 \end{bmatrix}\begin{bmatrix} \Delta r \\ \Delta \psi \end{bmatrix} + \begin{bmatrix} 1/I_{zz} \\ 0 \end{bmatrix}\Delta M_z \quad (7b)$$

Lateral Subsystem

$$\begin{bmatrix} \Delta\dot{p} \\ \Delta\dot{\phi} \\ \Delta\dot{v} \\ \Delta\dot{y} \end{bmatrix} = \begin{bmatrix} 0 & 0 & 0 & 0 \\ 1 & 0 & 0 & 0 \\ 0 & -g & 0 & 0 \\ 0 & 0 & 1 & 0 \end{bmatrix}\begin{bmatrix} \Delta p \\ \Delta \phi \\ \Delta v \\ \Delta y \end{bmatrix} + \begin{bmatrix} 1/I_{xx} \\ 0 \\ 0 \\ 0 \end{bmatrix}\Delta M_x \quad (7c)$$

Longitudinal Subsystem

$$\begin{bmatrix} \Delta\dot{q} \\ \Delta\dot{\theta} \\ \Delta\dot{u} \\ \Delta\dot{x} \end{bmatrix} = \begin{bmatrix} 0 & 0 & 0 & 0 \\ 1 & 0 & 0 & 0 \\ 0 & g & 0 & 0 \\ 0 & 0 & 1 & 0 \end{bmatrix}\begin{bmatrix} \Delta q \\ \Delta \theta \\ \Delta u \\ \Delta x \end{bmatrix} + \begin{bmatrix} 1/I_{yy} \\ 0 \\ 0 \\ 0 \end{bmatrix}\Delta M_x \quad (7d)$$

where $x = [x, y, z]$ represents the drone's linear position relative to a given inertially fixed reference frame, $\dot{x} = [u, v, w]$ represents the drone's linear velocity, $\theta = [\theta, \phi, \psi]$ represents the drone's angular position, and $q = [q, p, r]$ represents the drone's angular velocity.
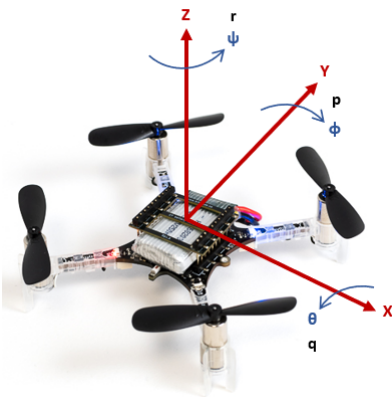

Figure 2: Noninertial Drone Body Fixed Frame.

Inputs to these state space realizations are a pulse width modulation (PWM) signal which controls the voltage sent to each direct current (DC) motor, raging from 0 to 65535,

which can be related to the motor rotations per minute (RPM) by the following linear relationship [19]:

$$\text{RPM} = 0.2685 * \text{PWM} + 4070.3 \quad (8)$$

The `gym-pybullet-drones` gym environment is equipped with a proportional-integral-derivative (PID) controller based on a version of the snap trajectory controller in [20], also commonly referred to as a Mellinger controller type in some literature [21], [22]. This architecture differs from the more common cascaded attitude-position controller by relaxing small pitch (θ) and roll (ϕ) drone attitude assumptions. The control architecture used in simulation is shown in Fig. 3.
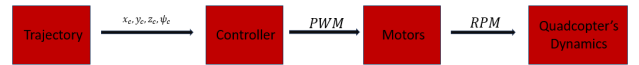

Figure 3: Crazyflie Simulation Control Architecture.

3. EXPERIMENTAL SETUP

This section describes the physical laboratory setup and Crazyflie drone swarming and waypoint following capabilities.

Laboratory Setup

The implementation considered in this paper is scaled to and designed for a 4x3x2.5 [m][1] flight volume, illustrated

[1]Note - The full lab space is 13x20x8 ft [23], but the space available for use with the lighthouse positioning system is 13x10x8 ft*

Drone Variables		
	I_{xx} [kg m^2]	1.4e-5
Moments	I_{yy} [kg m^2]	1.4e-5
	I_{zz} [kg m^2]	2.17e-5
Mass	m [kg]	0.027

Table 1: Listed variables used in linearized Craziefly 2.1 subsystems.
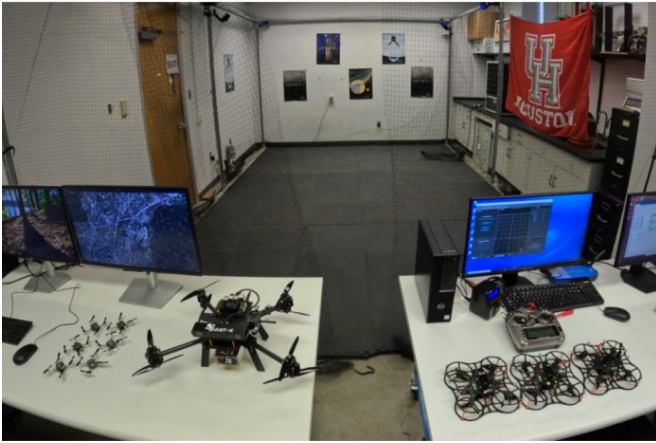
Figure 4: Advanced Learning, Artificial Intelligence, and Control Flight Arena at the University of Houston
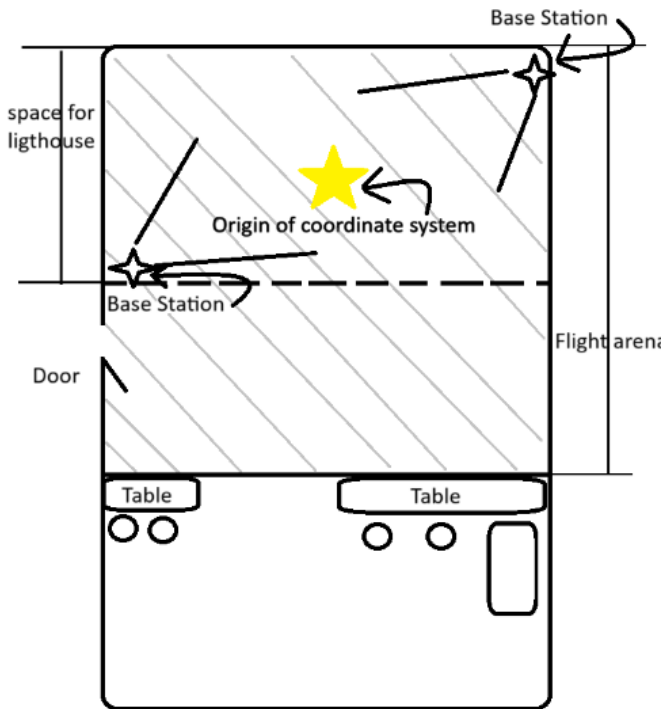
Figure 5: Diagram of Flight Arena

in Figs. 4-5. This lab setup includes a positioning system with two diagonally opposed Bitcraze Lighthouse V2 Base Stations [24]. These base stations operate by sending sweeps of infrared light that are observed by a Lighthouse deck on the Crazyflie. The Crazyflie uses the angles of these light sweeps to calculate its own position, which can then be communicated for use in a position/attitude controller via the Crazyradio system [24].

Swarm Capabilities

The Crazyflie platform has support for running swarms. The process for doing so is as follows:

1. The Uniform Resource Identifier (URI) (address) for communicating with each Crazyflie must be uniquely specified.

Figure 6: Workflow Block Diagram

2. Then, each trajectory is defined, paired to a drone's URI, and the swarm will follow the trajectories.

Waypoint Simulation Following on Crazyflies

The Lighthouse positioning system allows for the use of a global coordinate system with the origin set to the ground at the center of the flight space, with base units for distance in millimeters [24] [25] [26]. The trajectories and following waypoints are all made using a near identical global coordinate system with base units of meters. Scaling is performed to adjust the satellite trajectory to be flown on a Crazyflie.

4. SIMULATION SETUP

Overview

In this section, we present tests falling under two categories: spacecraft trajectory following and neural network control output following. In the first category, natural motion and controlled spacecraft trajectories governed by the linearized CW equations in Hill's frame are calculated, formatted, scaled in time and distance, and followed by Crazyflies. Next, reinforcement learning-based neural network control systems trained for docking scenarios are used to generate closed loop control outputs that are scaled in distance and time and simulated by the Crazyflie drones.

Testing Spacecraft Trajectory Following

The process of converting space dynamics to the terrestrial Crazyflie surrogates in simulation is depicted by the block diagram in Fig.6. First, the trajectory of the spacecraft under CW dynamics is calculated in the form of waypoints for spacecraft to follow. Second, this spacecraft trajectory is scaled in distance to an appropriate size to be flown on a Crazyflie 2.1 within the laboratory space and the duration is shortened to represent the entire path well within the battery life of the Crazyflie. Third, the gym environment is initialized and the waypoints are sent to the Crazyflie. Crazyflie tracking commands are generated using the PID controller introduced in Sec. 2 [20]. Fourth, a Crazyflie flight following these waypoints is simulated using the PID control commands. These steps are described in more detail in the following subsections.

Space Dynamics Simulator—Before being simulated on the Crazyflie surrogate, a spacecraft's motion in the space-scale Hill's frame is determined. The continuous form of the CW equations introduced in Eq. (1), were solved using a Runge-Kutta 45 solver. Note that the output is formatted such that the orbital period and simulation runtime are adjustable independently from each other. The spacecraft dynamics simulators were created as waypoint generating functions which convert the space-scale outputs of the Clohessy-Wiltshire solutions to the drone-scale and integrates into the existing trajectory input tools available in `gym-pybullet-drones`.

Waypoint Generation—Depending on the time span and the solver step size chosen, the simulator generates a number of waypoints for the simulated drone to follow. Before the

waypoints are sent to the simulator, the distance is scaled from the space-scale to the lab-scale, where the lab space is assumed to not be any larger than 4x3x2.5 meters. The distance scale is a factor of 4e3. The waypoints generated serve as discrete position inputs for the drone simulation system, where the number of waypoints solved correlates to the control frequency multiplied by the chosen time period. Fig.7 shows an example of the waypoints generated for an in-plane NMT where both the chief and the target remain in the same relative orbital plane (the z-axis, in this and future examples). The type of trajectory generated by the Clohessey-Wiltshire equations are dependent on the initial states of the system. The initial conditions used in this example are as follows:

$$x = 800 \quad \dot{x} = 0.16$$

$$y = \frac{2\dot{x}}{n} \quad \dot{y} = -2nx \tag{9}$$

$$z = 0 \qquad \dot{z} = 0$$

with x, y, z [m] and $\dot{x}, \dot{y}, \dot{z}$ [m/s]. These initial conditions were arbitrarily chosen to loosely model in-space/on-orbit servicing, assembly, and manufacturing (OSAM/ISAM) servicing between two bodies [27]. This simplified simulator was used to generate NMTs and completely makes up the 'Spacecraft Dynamics' block in Fig.6.

Tracking Commands—The drone's initial position is chosen to equal the lab-scale initial positions in the space dynamics simulator with the starting rotational position $\theta_0 = [0, 0, \pi/2]^T$ relative to the origin. This initial rotational position starts the drone with all four propellers facing upwards. The simulated drone acts as the deputy spacecraft surrogate and the origin of the inertially fixed frame as the chief. The generated waypoints are then injected into the flight simulator where the drone is controlled by the PID controller introduced in Section 2.

Space Dynamics Through Neural Network

An alternative method of generating a trajectory in the space-scale is through the use of a neural network control sys-
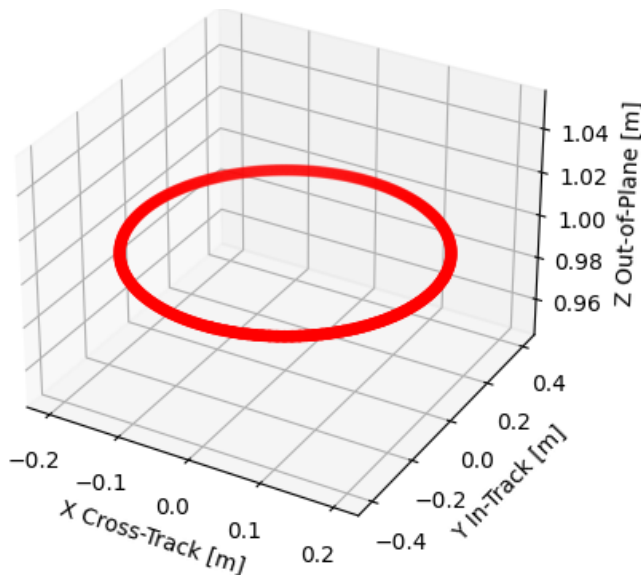
tem trained with reinforcement learning for specific on-orbit scenarios (e.g. docking and inspection) provided by the work outlined in [28]. In this implementation, the trained neural network outputs control the thrusts to the simulation with linearized Clohessy-Wiltshire equations that govern the satellite motion. This neural network controlled trajectory is then formatted and scaled to be flown on Crazyflies, the process for which is shown in Figure 8.
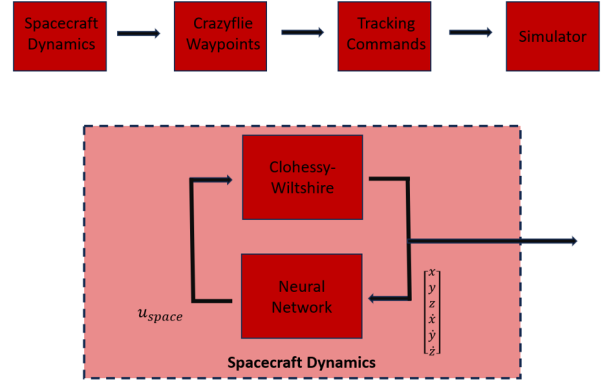

Figure 8: Workflow Block Diagram with Neural Network

5. RESULTS

Figures 9-10 show results of the waypoint trajectory tracking with the PID controller performed on an in-plane NMT in the gym environment. This simulated experiment was performed over the span of three complete orbital revolutions during a time span of ten seconds, with initial conditions previously introduced in Eq. 9.

A more general case of a relative elliptical orbit is that of out-of-plane trajectories where the follower and target satellite orbit in different orbital planes relative to the earth centered
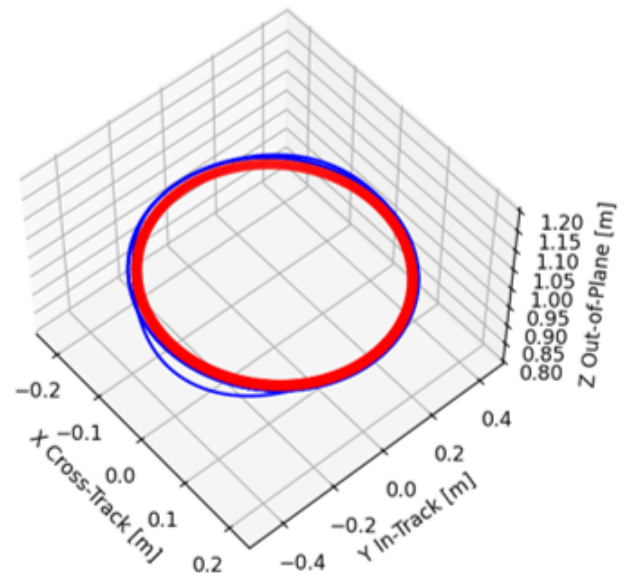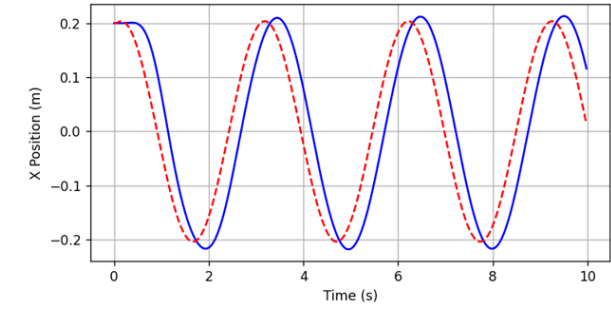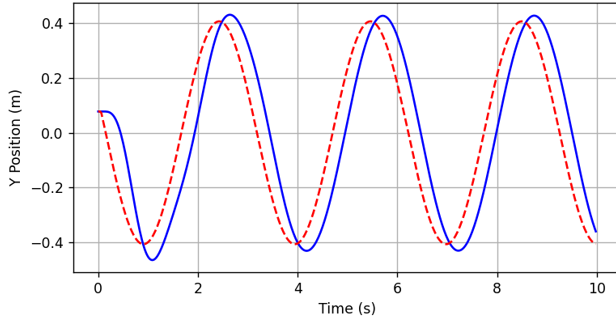

Figure 7: Lab-Scale, In-Plane Natural Motion Trajectory

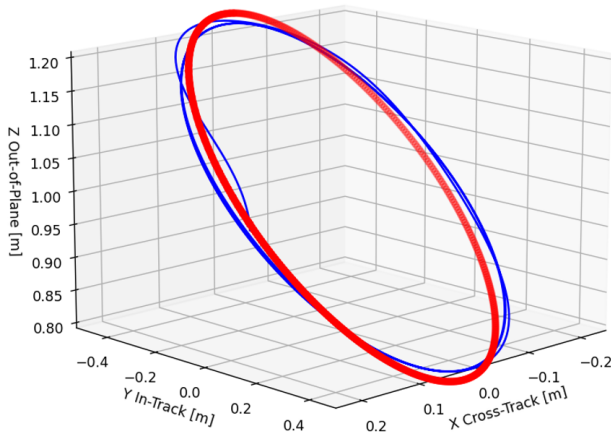**Figure 9**: 3D Plot of In-Plane Waypoint Tracking with Tuned PID

Figure 10: Drone X (a) and Y (b) Positions (Blue) Compared to Waypoints (Red)

frame. In order to create an out of plane elliptical NMT, the position and velocity initial conditions in the x and y axis remained the same as the previous case with the position and velocity in the z axis becoming non-zero. Arbitrary values were assigned to the states in the z axis,

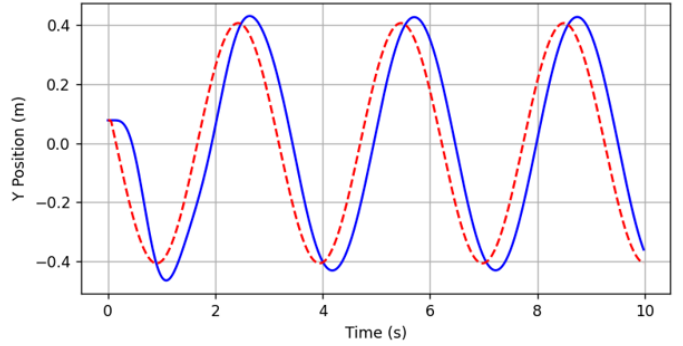$$z = 1 \quad \dot{z} = 1 \tag{10}$$

and the NMT generated was simulated in the gym environment. Results of this simulated experiment are given in Figs. 11-12.
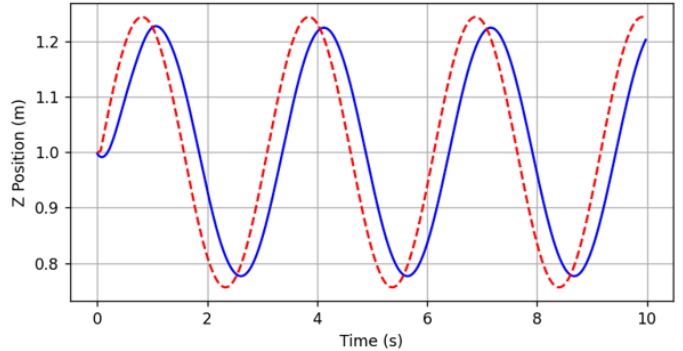

**Figure 11**: 3D Plot of Out-of-Plane Waypoint Tracking with Tuned PID
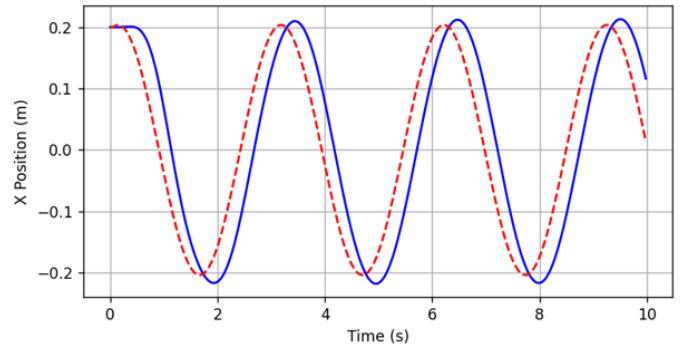
Figure 12: Drone X (a), Y (b), and Z (c) Positions (Blue) Compared to Waypoints (Red) for Out-of-Plane NMT

As explained in the previous section, the origin is representative of a target satellite and the trajectory shown is the chaser's trajectory relative to the target.

Crazyflie Tracking Reinforcement Learning Outputs

A trained reinforcement learning neural network [29] for a spacecraft docking scenario was inserted into the control scheme, as depicted in Figure 8, where the control thrusts from the trained neural network controller were fed into the Clohessy-Wiltshire linearized model, Eq. 1. A pre-generated trajectory for a docking scenario from this neural network was saved as a dictionary and was used as the input trajectory in the gym environment. In this scenario, a chaser spacecraft attempts to dock with a target spacecraft (located at the origin in the non-inertial Hill's frame) within a given time horizon. A simulation time horizon of 10 seconds was chosen and the docking scenario was simulated in the gym environment, the results of which can be seen in Figure 13 and Figure 14.
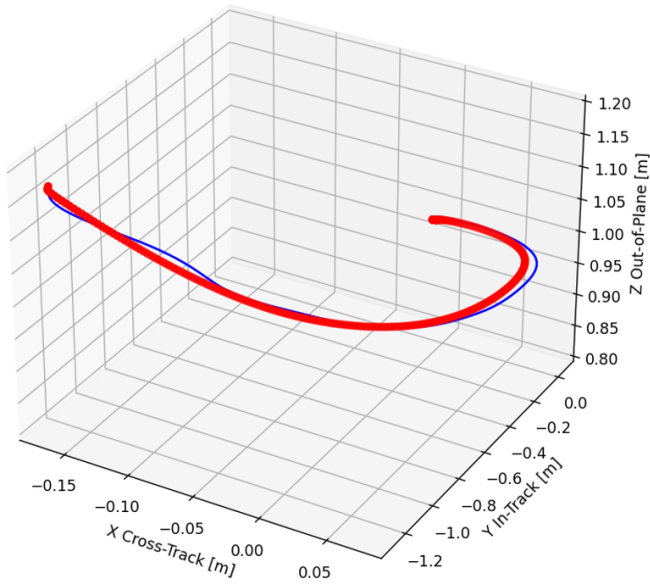
Figure 13: 3D Plot of RL-Trained Docking Simulation, Target Spacecraft is Assumed to be at coordinates [0,0,1]

A different neural network was trained for this same scenario and, instead of the trajectory generated being externally saved, the neural network control scheme was fully integrated with the `gym-pybullet-drones` simulator. The neural network can be trained with assigned values for the chief initial conditions. For this network, the initial conditions for the chief were chosen to all equal zero. Once trained, the neural network can control the deputy satellite to dock from a range of initial conditions chosen by a random number generator (RNG) with a seeded value. The initializer used for this scenario includes a built-in safety feature which ensures that the initial velocity of the deputy spacecraft does not violate a set maximum velocity safety limit (there exits a limit in which docking cannot be conducted safely). Figure 15 and Figure 16 show an implementation with a unique set of initial conditions. Note that the time horizon for this example was expanded to 14 seconds.

6. CONCLUSIONS

The capabilities of the Bitcraze's Crazyflie platform in testing satellite autonomy terrestrially were demonstrated in simulation. Simple relative satellite motion governed by the linearized Clohessy-Wiltshire equations in Hill's frame were fully implemented for testing simple in-plane and out-of-plane natural motion trajectories. Additionally, two tests of reinforcement learning controlled docking scenarios were successfully performed. The first RL agent's test was ran by saving the output of the RL agent's controlled flight, formatting it to be flown on the Crazyflies, then simulated. The second RL agent calculated the trajectory which was then directly formatted and flown by the Crazyflie in the gym environment.

Future Work

The next step in this research is translating the work completed in the `gym-pybullet-drones` simulation space to physical flight arena using actual Crazyflie drones. It is anticipated that a challenge in this transfer is the Sim2Real Correlation Coefficient (SRCC), a measure of how well a


(a)

(b)

(c)
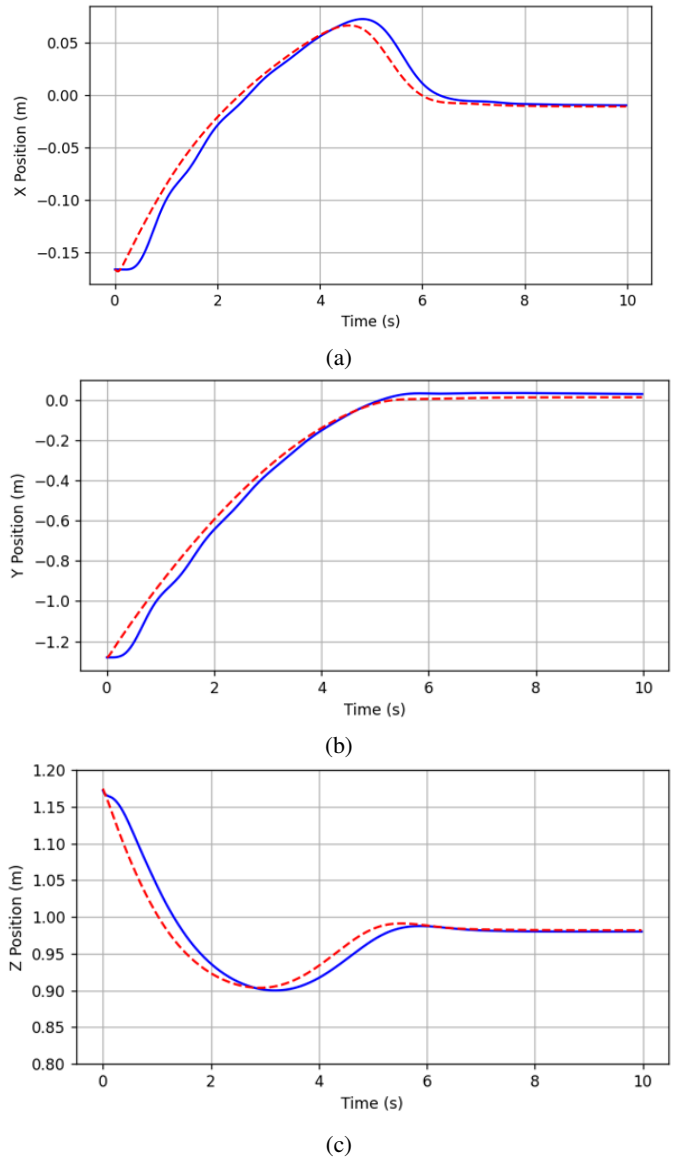
Figure 14: Drone X (a), Y (b), and Z (c) Positions (Blue) Compared to Waypoints (Red) for RL-Trained Docking Simulation

simulation matches real-world performance, which has not been extensively tested for `gym-pybullet-drones`. Imperfect models of aerodynamic effects, latency, and actuator saturation all impact this coefficient and may be reviewed. Additionally, the base PID controller can be further tuned to reduce any tracking error encountered in the simulation. When successfully physically implemented, this research may have a variety of use cases including testing novel inspection techniques of uncooperative target satellites [30] and cubesat proximity operations [31]. Visualizing physical performance of these types of missions can aid in evaluation and serve as a foundation for tuning.
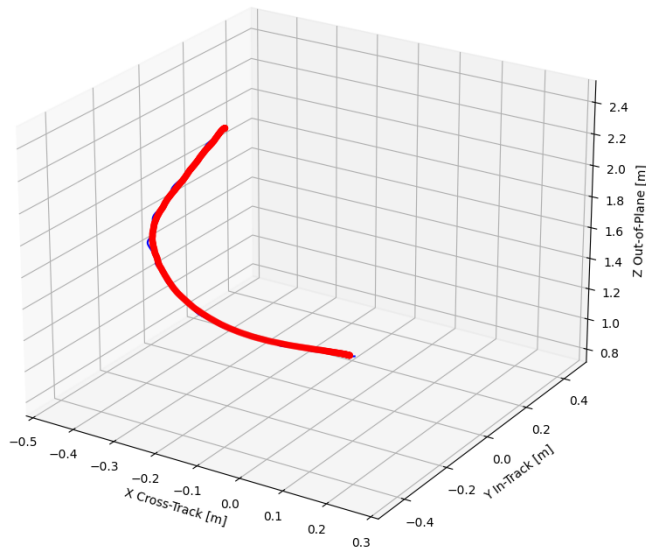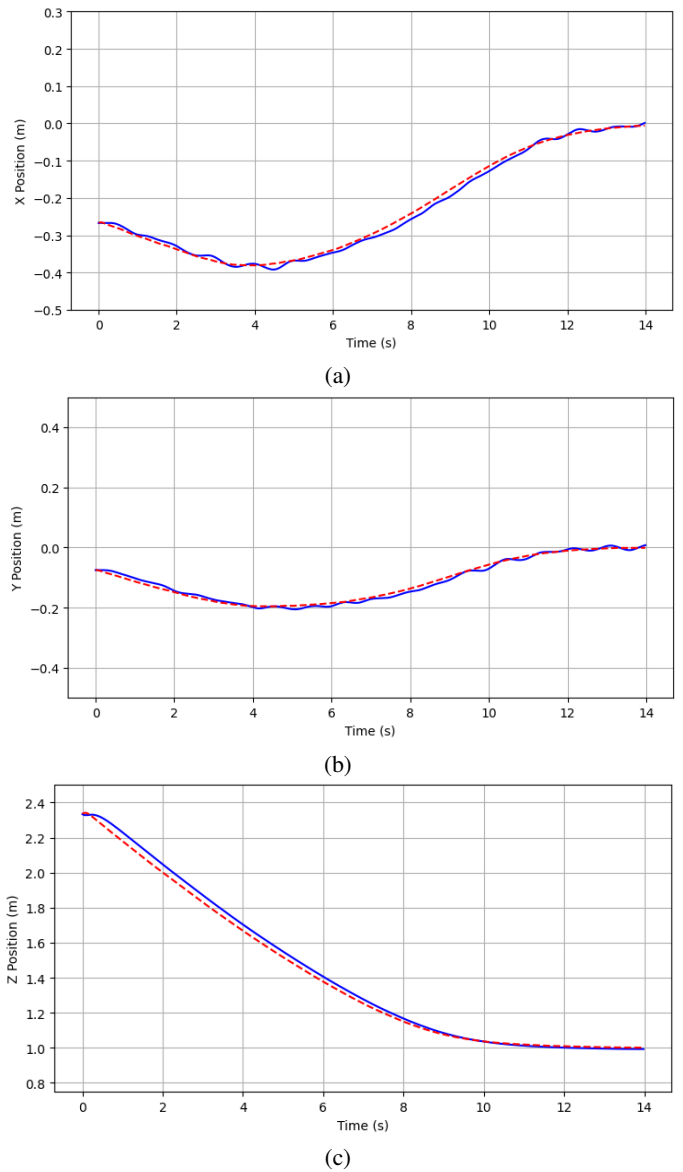
Figure 15: 3D Plot of Integrated RL Docking Simulation, Target Spacecraft is Assumed to be at coordinates [0,0,1]

Figure 16: Drone X (a), Y (b), and Z (c) Positions (Blue) Compared to Waypoints (Red) for Integrated RL Docking Simulation

REFERENCES

[1] S. Bandyopadhyay, G. P. Subramanian, R. Foust, D. Morgan, S.-J. Chung, and F. Hadaegh, "A review of impending small satellite formation flying missions," in *53rd AIAA Aerospace Sciences Meeting*, 2015, p. 1623.

[2] D. Piskorz and K. L. Jones, "On-orbit assembly of space assets: A path to affordable and adaptable space infrastructure," *The Aerospace Corporation*, pp. 12–13, 2018.

[3] G. Slater, S. M. Byram, and T. Williams, "Collision avoidance for satellites in formation flight," *Journal of guidance, control, and dynamics*, vol. 29, no. 5, pp. 1140–1146, 2006.

[4] N. Petit, M. Milam, and R. Murray, "Constrained trajectory generation for micro-satellite formation flying," in *AIAA Guidance, Navigation, and Control Conference and Exhibit*, 2001, p. 4030.

[5] T. Campbell, R. Furfaro, R. Linares, and D. Gaylor, "A deep learning approach for optical autonomous planetary relative terrain navigation," *Spaceflight Mechanics*, vol. 160, pp. 3293–3302, 2017.

[6] H. H. Lei, M. Shubert, N. Damron, K. Lang, and S. Phillips, "Deep reinforcement learning for multi-agent autonomous satellite inspection," in *44th Annual AAS Guidance, Navigation and Control (GN&C) Conference, Breckenridge, CO*, 2022.

[7] D. Pickem, L. Wang, P. Glotfelter, Y. Diaz-Mercado, M. Mote, A. Ames, E. Feron, and M. Egerstedt, "Safe, remote-access swarm robotics research on the robotarium," *arXiv preprint arXiv:1604.00640*, 2016.

[8] D. Pickem, P. Glotfelter, L. Wang, M. Mote, A. Ames, E. Feron, and M. Egerstedt, "The robotarium: A remotely accessible swarm robotics research testbed," in *2017 IEEE International Conference on Robotics and Automation (ICRA)*. IEEE, 2017, pp. 1699–1706.

[9] K. Hovell and S. Ulrich, "Deep reinforcement learning for spacecraft proximity operations guidance," *Journal of spacecraft and rockets*, vol. 58, no. 2, pp. 254–264, 2021.

[10] Z. S. Lippay, M. Shubert†, D. Baker, A. A. Soderlund, and S. Phillips, "Emulation of close-proximity spacecraft dynamics in terrestrial environments using unmanned aerial vehicles," in *AIAA SciTech 2024 Forum*, 2024, pp. 1–12.

[11] "Crazyflie 2.1," 2023, accessed on July 28, 2023. [Online]. Available: https://www.bitcraze.io/products/crazyflie-2-1/

[12] W. Giernacki, M. Skwierczyński, W. Witwicki, P. Wroński, and P. Kozierski, "Crazyflie 2.0 quadrotor as a platform for research and education in robotics and control engineering," in *2017 22nd International Conference on Methods and Models in Automation and Robotics (MMAR)*. IEEE, 2017, pp. 37–42.

[13] J. Panerati, H. Zheng, S. Zhou, J. Xu, A. Prorok, and A. P. Schoellig, "Learning to fly—a gym environment with pybullet physics for reinforcement learning of multi-agent quadcopter control," in *2021 IEEE/RSJ International Conference on Intelligent Robots and Systems (IROS)*. IEEE, 2021, pp. 7512–7519.

[14] K. Himanshu, J. V. Pushpangathan *et al.*, "Waypoint navigation of quadrotor using deep reinforcement learning," *IFAC-PapersOnLine*, vol. 55, no. 22, pp. 281–286, 2022.

[15] J. Förster, "System identification of the crazyflie 2.0 nano quadrocopter," B.S. thesis, ETH Zurich, 2015.

[16] W. Clohessy and R. Wiltshire, "Terminal guidance system for satellite rendezvous," *Journal of the aerospace sciences*, vol. 27, no. 9, pp. 653–658, 1960.

[17] G. W. Hill, "Researches in the lunar theory," *American journal of Mathematics*, vol. 1, no. 1, pp. 5–26, 1878.

[18] Y. K. Nakka, W. Hönig, C. Choi, A. Harvard, A. Rahmani, and S.-J. Chung, "Information-based guidance and control architecture for multi-spacecraft on-orbit inspection," *Journal of Guidance, Control, and Dynamics*, vol. 45, no. 7, pp. 1184–1201, 2022.

[19] C. Luis and J. L. Ny, "Design of a trajectory tracking controller for a nanoquadcopter," *arXiv preprint arXiv:1608.05786*, 2016.

[20] D. Mellinger and V. Kumar, "Minimum snap trajectory generation and control for quadrotors," in *2011 IEEE international conference on robotics and automation*. IEEE, 2011, pp. 2520–2525.

[21] A. El Asslouj and H. Rastgoftar, "Quadcopter tracking using euler-angle-free flatness-based control," in *2023 European Control Conference (ECC)*. IEEE, 2023, pp. 1–6.

[22] A. Javeed, V. L. Jiménez, and J. Grönqvist, "Reinforcement learning-based control of crazyflie 2. x quadrotor," *arXiv preprint arXiv:2306.03951*, 2023.

[23] M. Cescon, "Flight arena," 2023, accessed on July 13, 2023. [Online]. Available: https://cescon.me.uh.edu/facilities/

[24] A. Taffanel, B. Rousselot, J. Danielsson, K. McGuire, K. Richardsson, M. Eliasson, T. Antonsson, and W. Hönig, "Lighthouse positioning system: dataset, accuracy, and precision for uav research," *arXiv preprint arXiv:2104.11523*, 2021.

[25] Bitcraze, "Generic setpoint crtp port," 2023, accessed on July 13th, 2023. [Online]. Available: https://www.bitcraze.io/documentation/repository/crazyflie-firmware/master/functional-areas/crtp/

[26] ——, "The coordinate system of the crazyflie 2.x," 2023, accessed on July 13, 2023. [Online]. Available: https://www.bitcraze.io/documentation/system/platform/cf2-coordinate-system/

[27] D. Arney, R. Sutherland, J. Mulvaney, D. Steinkoenig, C. Stockdale, and M. Farley, "On-orbit servicing, assembly, and manufacturing (osam) state of play," 2021.

[28] N. Hamilton, K. Dunlap, T. T. Johnson, and K. L. Hobbs, "Ablation study of how run time assurance impacts the training and performance of reinforcement learning agents," *arXiv preprint arXiv:2207.04117*, 2022.

[29] U. J. Ravaioli, J. Cunningham, J. McCarroll, V. Gangal, K. Dunlap, and K. L. Hobbs, "Safe reinforcement learning benchmark environments for aerospace control systems," in *2022 IEEE Aerospace Conference (AERO)*. IEEE, 2022, pp. 1–20.

[30] D. van Wijk, K. Dunlap, M. Majji, and K. L. Hobbs, "Deep reinforcement learning for autonomous spacecraft inspection using illumination," *arXiv preprint arXiv:2308.02743*, 2023.

[31] J. Bowen, M. Villa, and A. Williams, "Cubesat based rendezvous, proximity operations, and docking in the cpod mission," 2015.

Arturo de la Barcena III *is an intern working under Dr. Kerianne Hobbs and a mechanical engineering master's student at the University of Houston. His primary research interests are in air and space vehicle control and autonomy and has been involved with the Advanced Learning, Artificial Intelligence and Control lab at the University of Houston for over two years.*

Collin J. Rhodes *is a contracted intern for the Air Force Research Lab working directly under Dr. Hobbs. He is a graduate student studying Mechanical Engineering with a focus in controls at the University of Houston. In addition to research and classes, Collin is also the President of Cougar Racing, a student organization wherein students compete against other universities in designing and building a race car every year.*

John McCarroll *is a Junior Autonomy Engineer on the Autonomy Capability Team (ACT3) at the Air Force Research Laboratory. He works on the Safe Autonomy team, supporting development efforts and experimenting with reinforcement learning. John received his BS degree in Software Engineering from Rochester Institute of Technology, where he gained experience in neural architecture search using genetic algorithms, CNNs applied to games and art, data warehousing, and data visualization.*

Marzia Cescon *is the David C. Zimmerman Assistant Professor of Mechanical Engineering at the University of Houston, Houston, TX. She is the founder and director of the Advanced Learning, Artificial Intelligence and Control laboratory, a multidisciplinary effort developing novel computational methods and tools for learning-based decision making and control of complex and unknown dynamical systems. Her interests span biomedical control systems, multi-agent systems, flight control and aerospace*

control, and safe autonomy. Dr. Cescon earned a Bachelor Degree in Information Engineering and a Master Degree in Control Systems Engineering both from the University of Padua, Italy, and received the Ph.D. degree in Automatic Control from the Automatic Control Department at Lund University, Sweden. She has held several research positions including at the University of California, Santa Barbara, the Melbourne School of Engineering at University of Melbourne, and the Harvard John A. Paulson School of Engineering and Applied Sciences at Harvard University.

***Kerianne L. Hobbs** is the Safe Autonomy and Space Lead on the Autonomy Capability Team (ACT3) at the Air Force Research Laboratory. There she investigates rigorous specification, analysis, bounding, and intervention techniques to enable safe, trusted, ethical, and certifiable autonomous and learning controllers for aircraft and spacecraft applications. Her previous experience includes work in automatic collision avoidance and autonomy verification and validation research. Dr. Hobbs was selected for the 2020 AFCEA 40 Under 40 award and was a member of the team that won the 2018 Collier Trophy (Automatic Ground Collision Avoidance System Team), as well as numerous AFRL Awards. Dr. Hobbs has a BS in Aerospace Engineering from Embry-Riddle Aeronautical University, an MS in Astronautical Engineering from the Air Force Institute of Technology, and a Ph.D. in Aerospace Engineering from the Georgia Institute of Technology.*